ACS APPLIED MATERIALS & INTERFACES

Research Article

www.acsami.org

Stabilizing Nanosized Si Anodes with the Synergetic Usage of Atomic Layer Deposition and Electrolyte Additives for Li-Ion Batteries

Sunny Hy,[†,∥] Yi-Hsiu Chen,[†] Ho-Ming Cheng,[†] Chun-Jern Pan,[†] Ju-Hsiang Cheng,[†] John Rick,[†] and Bing-Joe Hwang*[,†,‡]

[†]Nanoelectrochemistry Laboratory, Department of Chemical Engineering, National Taiwan University of Science and Technology, Taipei 106-07, Taiwan

[‡]National Synchrotron Radiation Research Center, Hsin-Chu 30076, Taiwan

Supporting Information

ABSTRACT: A substantial increase in charging capacity over long cycle periods was made possible by the formation of a flexible weblike network via the combination of Al_2O_3 atomic layer deposition (ALD) and the electrolyte additive vinylene carbonate (VC). Transmission electron microscopy shows that a weblike network forms after cycling when ALD and VC were used in combination that dramatically increases the cycle stability for the Si composite anode. The ALD−VC combination also showed reduced reactions with the lithium salt, forming a more stable solid electrolyte interface (SEI) absent of fluorinated silicon species, as evidenced by X-ray photoelectron spectroscopy. Although the bare Si composite anode showed only an improvement from a 56% to a 45% loss after 50 cycles, when VC was introduced, the ALD-coated Si anode showed an improvement from a 73% to a 11% capacity loss. Furthermore, the anode with the ALD coating and VC had a capacity of 630 mAh g^{-1} after 200 cycles running at 200 mA g^{-1}, and the bare anode without VC showed a capacity of 400 mAh g^{-1} after only 50 cycles. This approach can be extended to other Si systems, and the formation of this SEI is dependent on the thickness of the ALD that affects both capacity and stability.

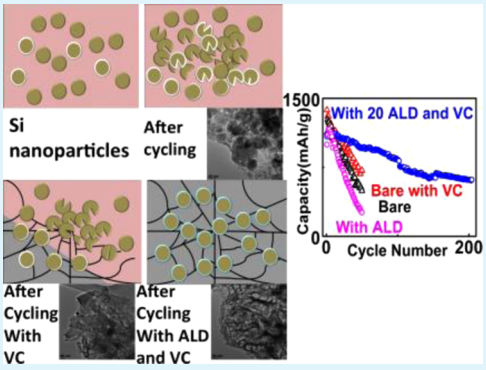

KEYWORDS: *silicon, anode, lithium battery, composite, carbon, additive*

1. INTRODUCTION

Silicon, a naturally abundant element, is one of the more promising candidates for low-cost, high-theoretical capacity (4200 mAh/g) Li-ion battery (LIB) electrodes.[1] However, unlike commercial carbon anodes (372 mAh/g), silicon undergoes huge stress-inducing volume changes (around 300%) that lead to the formation of cracks. These cracks may electrochemically isolate individual particles, thus facilitating the formation of a continuous solid electrolyte interface (SEI) and leading to a diminished capacity with repeated cycling.[2] Silicon nanoparticle−carbon composites have been developed that alleviate these problems by dispersing the silicon nanoparticles using a mixture of various forms of carbon, including amorphous carbon, graphene sheets, and carbon nanotubes.[1] The dispersion of silicon within this composite material provides free space for "cushioning", thus mitigating the effects of the nanoparticle expansion while at the same time allowing for a more homogeneous lithiation−delithiation with both an improved rate capability and an increased conductivity.[3] Although cracks related to volume expansion are minimized to a great extent when a composite mixture is used, issues related to SEI cracking are still present.[2,4] In an effort to further improve cycle stability, an artificial SEI was made by the atomic layer deposition (ALD) of an Al_2O_3 coating directly onto the Si composite anode and the subsequent electrochemical reaction of this electrode with the electrolyte additive vinylene carbonate (VC, 2 wt %) during charging and discharging. This forms a stable weblike SEI matrix that showed improved stability compared to that of the bare Si composite anode. Unlike other coating methods,[5] ALD coatings can be directly applied to the electrode, thus obviating the need to first apply to an anode powder. Furthermore, ALD coating is a very mild approach that allows the controlling of coating thicknesses to several angstroms with good uniformity.[6−8] VC, due to its stability-enhancing capabilities, was used in conjunction with ALD coating.[9−12]

Here, we discuss the development of the artificial SEI that was able to protect the silicon nanoparticle surface from reaction with the electrolyte and thus maintain the overall nanoparticle dispersion. Unlike similar coating methods, this method can be adapted to silicon-containing systems to improve the capacity retention.

Received: March 2, 2015
Accepted: May 19, 2015
Published: May 19, 2015

DOI: 10.1021/acsami.5b01853
ACS Appl. Mater. Interfaces 2015, 7, 13801−13807

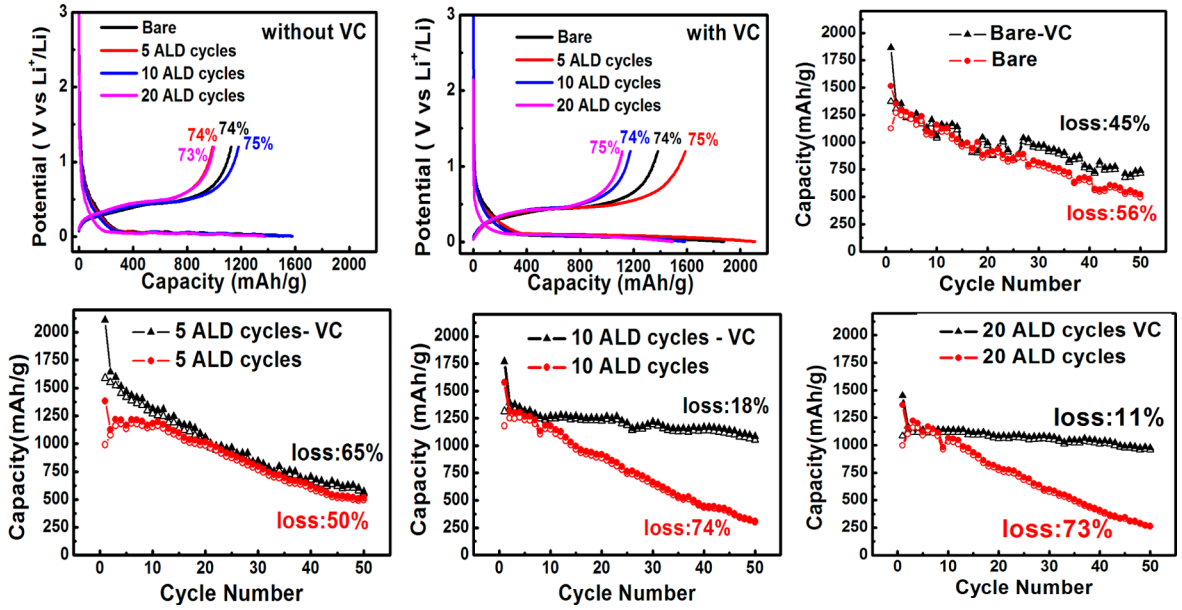

Figure 1. Electrochemical charge−discharge curves for the different Al_2O_3 ALD-coated Si−C anodes with (top center) and without (top left) VC additive. Capacity versus cycle number for bare (top right), 5 Al_2O_3−ALD- (bottom left), 10 Al_2O_3−ALD- (bottom center), and 20 Al_2O_3−ALD-coated (bottom right) Si−C anodes with and without VC additive.

2. EXPERIMENTAL SECTION

Si/rGO/CNT Composite Synthesis and ALD Coating. The preparation of nanosized silicon was similar to that in previous reports.[3,13,14] Briefly, nanosized silicon was first treated in a solution of 5% HF for 1 h to eliminate surface oxides and then filtered. A total of 300 mg of silicon and 1.64 g of 4-aminobenzoic acid were then dispersed in 60 mL of acetonitrile. A total of 5 ml of isoamyl nitrite was then injected into the solution and continuously stirred and heated at 70 °C under N_2 gas purging for 24 h. The silicon was then filtered, cleaned with DI water, and dried within a vacuum oven. The chemical oxidation of carbon nanotubes (CNT) was done by suspending the CNT in a solution of H_2SO_4/HNO_3 (3:2) and continuously stirred and heated at 80 °C for 4 h under Ar gas purging. The solution was centrifuged to concentrate the solution and then brought to a neutral pH by dialysis. Graphene oxide (GO) was prepared by the improved Hummers method.[15] Nanosized silicon and CNT was then added to the GO suspension in H_2O with a weight ratio of 2:0.5:0.5 of Si/CNT/GO. The mixture was then freeze-dried and subsequently reduced for 1 h at 500 °C under 5% H_2 and 95% Ar gas in a tubular furnace. Electrode fabrication was done by first forming a slurry of the Si−C composite (Super P conductive carbon and poly(acrylic acid) (PAA, average MW of approximately 10 000 g/mol), weight ratio 80:10:10 in DI H_2O). The slurry was then cast over a Cu foil and dried at 60 °C overnight. The loading of active material was approximately 2 mg/cm^2. Al_2O_3 films were grown directly on the Si−C electrodes. The precursors used for the Al_2O_3 ALD were water and trimethylaluminum [(TMA), $Al(CH_3)_3$], with a processing temperature of 200 °C and Ar purging at 0.5 Torr using the ALD system implemented by the Kao Duen Technology Corporation. The thickness of the ALD coating for each ALD cycle was estimated to be approximately 0.1 nm per cycle using a silicon substrate in which 5, 10, and 20 ALD cycles correspond to ∼0.5, 1, and 2 nm, respectively.

Electrochemical Characterization and Material Characterization. Half-cell coin cell batteries were assembled in an Ar-filled glovebox using Li foil as a counter electrode with 1 M $LiPF_6$ in ethylene carbonate/diethyl carbonate (EC/DEC) 1:1 electrolyte with and without the addition of 2 wt % vinylene carbonate. The charge−discharge capacity of the assembled coin cell was recorded with a battery testing system (Maccor series 4000). The coin cell was charged and discharged galvanostatically at a rate of 200 mA/g in the potential window of 1.2−0.005 V corresponding to a deep discharge. For postcycling analysis, electrodes were prepared by extracting the electrodes from the coin cell in an Ar-filled glovebox and washing them gently with DEC. Extracted electrodes were maintained in an inert atmosphere before transferring; the transferring time was kept to a minimum. The surface morphologies of the synthesized powders and electrodes were examined using scanning electron microscopy (JEOL, JSM 6500). Transmission electron microscopy (TEM) was performed on a FEI-TEM-2000 microscope operated at an accelerating voltage of 3800 V on which the extracted electrode material was dispersed on a copper grid with lacy carbon. X-ray photoelectron spectroscopy (XPS) was performed at the BL24A1 Wide Range SGM beamline (with a bending magnet source that delivers photons over the range of 10 to 1500 eV) of the National Synchrotron Radiation Research Center (NSRRC) at Hsinchu, Taiwan. An excitation energy of 800 eV was used.

3. RESULTS AND DISCUSSION

Figure 1 shows the electrochemical charging−discharging curve (top left and middle) and capacity versus cycle number that compares electrodes formed with ALD cycling in conjunction with, and in the absence of, VC. Although the first cycle's efficiency shows little to no change with the addition of VC for each electrode, the charge capacity shows a noticeable increase. In particular, the bare electrode shows an increase from 1125 to 1350 mAh/g. An even more significant increase can be seen for the 5 ALD cycle electrode, in which the capacity increases from

DOI: 10.1021/acsami.5b01853
ACS Appl. Mater. Interfaces 2015, 7, 13801−13807

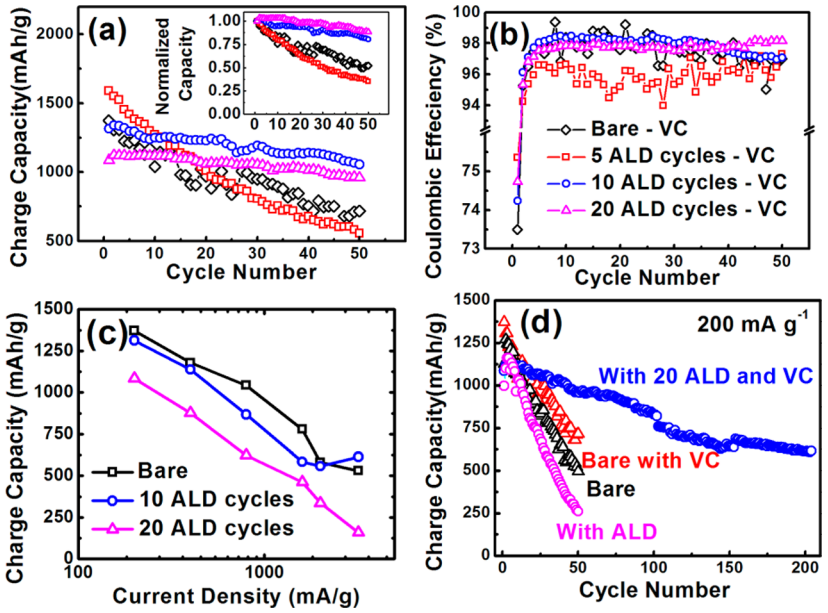

Figure 2. (a) Charging capacity versus cycle number of the different Al_2O_3 ALD cycles with VC additive (including an inset of the normalized capacity), (b) corresponding Coulombic efficiency, (c) charging capacity versus current density in log scale showing rate capability, and (d) the charging capacity versus cycle number of the bare and 20 ALD cycle electrodes with and without VC additive.

Table 1. Comparison of Other Silicon-Based Anodes Using Either ALD Coating or VC Additives

material	electrolyte[a]	coating	voltage (V)	C-rate[b]	cycles	capacity	retention (%)	ref.
Si nanotube	1:1:1 EC/DEC/DMC	TiO_2 ALD 1.5/1.5 nm	0.01−2	0.20	200	1700 mAh/g	60.2	8
Si@SIO_2/C	1:1 EC/DMC 2 wt % VC	a-C	0.05−1	0.04	60	1100 mAh/g	100.0	9
Si film	1:1 EC/DMC 1 wt % VC	N/A	0−1.5	N/A	500	20 μAh/cm^2	50.0	10
Si film	1:1 EC/DMC	Al_2O_3 ALD 20 Å	0.005−2	0.89	100	3000 mAh/g	75.0	17
Si film	1:1: EC/DEC	Al_2O_3 ALD 5 nm	0.001−2.5	10 μA	11	900 mAh/g	100.00	18
Si−graphene	1:1 EC/EMC	Al_2O_3 ALD 10 Å	0.01−1	0.10	400	701 mAh/g	70.95	19
Si−CNT−rGO	1:1 EC/DEC 2 wt % VC	Al_2O_3 ALD 20 Å	0.005−1.2	0.05	200	630 mAh/g	57.7	this work

[a]All have 1 M $LiPF_6$. [b]C = 4200 mAh/g unless specified.

1000 to 1600 mAh/g. The difference in charge capacity between the VC-containing and -noncontaining electrodes decreases with increasing ALD cycles, with only a difference of approximately 20 mAh/g when comparing the charge capacities of the 20 ALD cycle electrodes. This is related to the fast kinetics that have been previously observed with thinner ALD coatings on silicon thin film electrodes.[16] Interestingly, although 5 ALD coatings showed improved kinetics, the electrode's resulting stability was inferior to that of a bare electrode. Looking at the capacity versus the cycle number, with increasing cycle numbers a significant trend can be seen in stability with the combination of ALD and VC. After 50 cycles, the bare Si composite showed similar capacity losses of 45% and 56% for the VC-containing and -noncontaining electrodes, respectively. For 5 ALD cycles, the capacity loss is even higher for the VC-containing versus the -noncontaining battery, with 65% and 50% capacity loss, respectively. In comparison, 10 and 20 ALD cycles with VC show only an 18% and an 11% capacity loss, respectively. This is a significant improvement over the same electrodes without VC, with which there is a 74% and a 73% capacity loss after 50 cycles for the 10 and 20 ALD cycles, respectively. The capacity versus cycle number for the batteries containing only VC was further compared in Figure 2a. A trend can be observed in which increasing ALD cycles show an increasingly stable capacity retention (from 55% for the bare electrode to 89% for the 20 ALD treated electrode) but with a steady decline in the reversible charging capacity (1350 mAh g^{-1} for the bare electrode to 1090 mAh g^{-1} for first charge capacity of the 20 ALD treated electrode). The inset shows the normalized capacity, further illustrating the capacity retention trend. Figure 2b shows the corresponding Coulombic efficiencies. Only a slight improvement in the first cycle efficiency was observed for the ALD-coated electrodes versus that for the bare electrodes, but an improvement in the Coulombic efficiency across multiple cycles (a steady 98%) can be observed for the 10 and 20 ALD coatings compared to that of the bare electrode. However, the 5 ALD electrode showed unsteady charging and discharging, leading to inconsistent efficiencies from cycle to cycle and an average efficiency close to 95%. This unsteady efficiency could be related to the electrolyte interaction of the surface of the electrode with the thin ALD coating, where it is possible for the mechanical integrity of the thinner ALD coating, unable to withstand the silicon expansion with the addition of Al_2O_3, to further promote the formation of electrolyte reduction products. Another possibility may be a critical amount or critical thickness threshold before the interaction between the ALD coating and VC can take place. Figure 2c shows the rate capability of the bare, 10 ALD, and 20 ALD variations; no improvement was observed until higher rates for the 10 ALD variation were reached (2000 mA g^{-1} and above), and a drop in rate capability was noted for the 20 ALD variation (1600 mA g^{-1} and above).

DOI: 10.1021/acsami.5b01853
ACS Appl. Mater. Interfaces 2015, 7, 13801−13807

This is consistent with the observation of higher kinetics in Al_2O_3 ALD-coated Si thin films, in which the values from samples with up to 10 ALD cycles showed an improvement over those of the bare Si film and a slight drop in the rate capability at 20 ALD cycles and above.[16] These results show that the thickness of the ALD coating governs not only the rate capability but also the stability of the anode, due to the reaction with the electrolyte and the resulting SEI. The ALD−VC treatment serves primarily to stabilize the material, but the rate capability depends predominately on the initial composite material. Figure 2d shows the results of the electrode with 20 ALD cycles and VC (cycling up to 200 cycles at 200 mA g^{-1}), as well as those of the bare electrode with and without VC and of the 20 ALD cycle electrode without VC, enabling a comparison of cycle stability. Although most of the batteries showed a dramatic decay at 50 cycles, the 20 ALD cycle electrode with VC showed a capacity of 630 mAh g^{-1} even after 200 cycles (57.7% retention at 200 cycles compared to 43% at 50 cycles for the bare Si composite electrode). For comparison, Table 1 shows the electrochemical performance of several other silicon-based anode materials that have utilized ALD coating or VC additive electrolytes.[8−10,17−19] The C-rates listed in Table 1 are the rates during cyclability tests. Some works listed rates as mA g^{-1}, which were converted to C-rates assuming a theoretical capacity of 4200 mAh g^{-1} from $Li_{4.2}Si$; capacities are the capacity after the specified number of cycles. Although capacities and retentions are listed, voltage range and C-rate also have a large impact on the stability of the material; namely, a voltage-limiting discharge may lower the capacities but improve overall retention, and faster C-rates also show better retention compared to that of slower C-rates.[20] The silicon morphology and size also dictate how well the material cycles, making it difficult for the direct comparison of electrochemical performance. In any case, ALD coating or the addition of VC shows cycle retention above 50% for all of the materials after extended cycling and improvements compared to the retention for the respective bare electrodes or for the electrolyte without the addition of VC.

To observe the changes that occurred after electrochemical cycling, we extracted the bare, bare with VC, and ALD with VC electrodes from the coin cells for postcycling analysis.

Figure 3 shows images of the electrodes and corresponding separators after cycling in which the bare electrodes show white surface formations, and the initially white separator has become gray and black, due to the loss of anode material from the electrode to the separator resulting from the Si undergoing continuous expansion and cracking. The bare electrode with VC also shows white formations on its surface; however, the separator shows only slight signs of material loss from the electrode and has now become yellow due to VC-related reactions. The 20 ALD with VC electrode shows no white spots or other color variation, but the separator shows less greying from electrode material loss in comparison to the bare electrodes with and without VC. Figure 4 shows SEM (top) surface morphology images of the electrodes after cycling (an image of the electrode [Si−C anode] before cycling can be seen in Figure S2 in the Supporting Information) in which the bare electrode without VC shows that a SEI layer has formed with several rough ridges and cracks. The ALD-coated electrode with VC shows a much smoother and more consistent SEI form with fewer cracks. TEM images were also taken and can be seen at the bottom of Figure 4; the bare electrode without VC shows expanded Si particles, broken isolated pieces, and

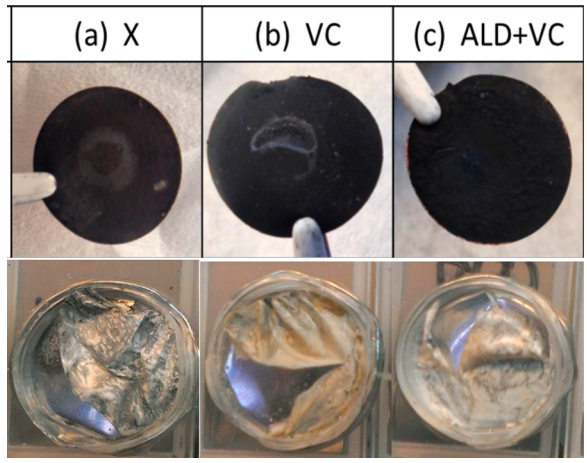

Figure 3. Images of the electrodes (top) and corresponding separator (bottom) of (a) the bare electrode without VC after 50 cycles (X), (b) the bare electrode with VC after 50 cycles (VC), and (c) the electrode with 20 ALD cycles and the addition of VC after 50 cycles (ALD−VC).

some clustering. With VC, the material changes are similar with the exception of a small weblike formation that can be observed at the bottom of the image as well as some semitransparent wormlike growths throughout. The ALD-coated electrode with VC also showed the weblike SEI formation but with greater consistency throughout the composite material; this may be related to the more consistent overall polymerization of VC. It is believed that this is related to altered interactions of the electrode's surface with the VC-containing electrolyte (catalyzed by the Al_2O_3 ALD coating) that may have effectively changed the surface of the electrode. The polymerlike species, observed with VC-containing electrolyte systems, is generally cohesive and flexible.[10,21] EIS measurements were performed to observe the changes relative to the effect of the combination of both ALD and VC. Figure 5 shows the impedance of the bare and 20 ALD electrode with VC after 50 cycles at the discharged state; both exhibit a high-frequency semicircle representing the SEI layer and a lower-frequency sloping line. Interestingly, a third semicircle can be observed between the low- and high-frequency elements within the bare electrode curve (but which is not apparent in the 20 ALD electrode curve) that may be attributed to either CNT or rGO. In any case, differences between the two impedance curves show that the addition of both VC and ALD in combination gives different SEI and charge transfer resistances. Recently, it has been shown that the interaction of the electrode's surface with the lithium salt (generally $LiPF_6$) generally leads to surface reactions that form species such as SiO_xF_y that prove to be devastating to the stability of the material.[22] Mitigating the formation of these species has been shown to significantly improve the stability.[23] XPS measurements were performed to look at the surface formation of the Si 2p of the bare and the ALD-coated electrodes with and without VC (Figure 6); similar to previous reports on silicon electrodes with EC/DEC 1:1 $LiPF_6$-based electrolytes,[22,23] the formation of SiO_xF_y can be observed on the bare electrode with or without VC, but the ALD-coated electrode shows only a slight formation of SiO_xF_y and SiO_2 in the absence of VC. ALD-coated electrodes with VC showed no clear SiO_xF_y formation (i.e., only SiO_2 formation), demonstrating its ability to mitigate reactions with $LiPF_6$. Only slight changes were observed for Al. Scheme 1 summarizes the

DOI: 10.1021/acsami.5b01853
ACS Appl. Mater. Interfaces 2015, 7, 13801−13807

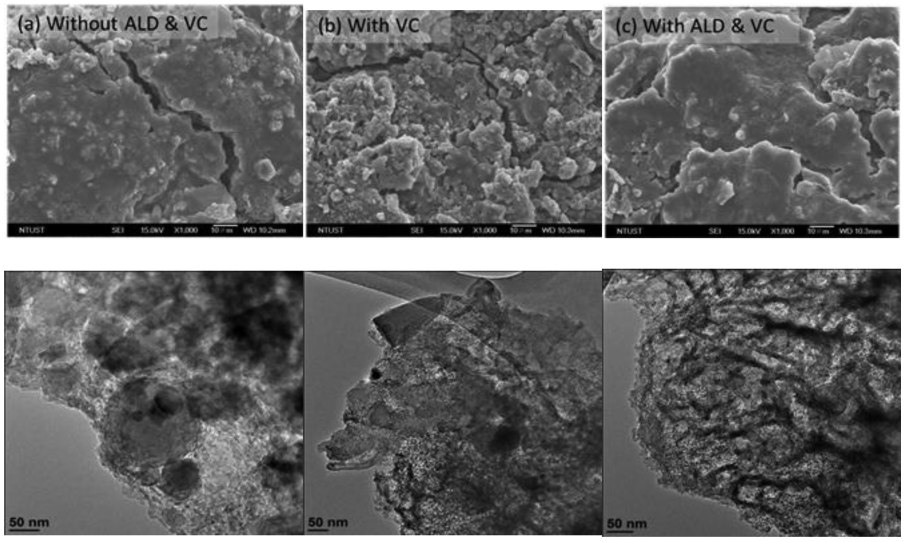

Figure 4. SEM (top) and TEM (middle) of the Si−C composite (a) without ALD and VC after 50 cycles, (b) with VC after 50 cycles , and (c) with ALD and VC after 50 cycles.

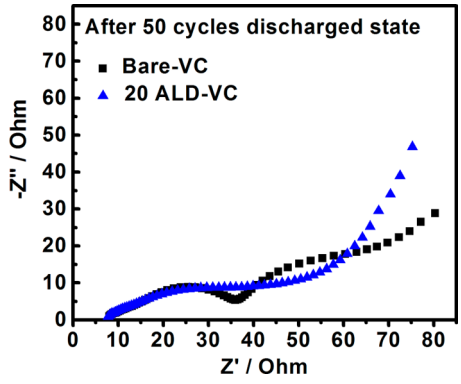

Figure 5. EIS measurements of the bare and 20 ALD electrodes with the addition of 2 wt % VC after 50 cycles at the discharged state.

observations found when a combination of ALD Al_2O_3 coating and 2 wt % VC is used in the Si composite anode. Before cycling, the silicon nanoparticles, if not ALD-coated, show some partial SiO_x surface formation that generally is unavoidable when the electrode is being fabricated or handled in ambient conditions. Upon cycling, there are three scenarios that occur depending on the specific ALD and VC combination. If there is no ALD coating or VC, the silicon nanoparticles tend to be pulverized due to the repeated expansion with lithiation, and the nanoparticles also tend to aggregate. In addition, the SEI also contains SiO_xF_y that decreases the stability. In the absence of ALD (but with VC), the silicon nanoparticles also undergo similar pulverization, aggregation, and SEI formation. However, a small portion of the electrode forms a weblike formation that may be initiated by the SiO_x surface formed on different particles. When ALD coating is applied with the addition of VC, a more stable SEI has formed that is absent of SiO_xF_y, with reduced pulverization of the nanoparticles and a weblike formation that keeps the particles from agglomerating. These results show the synergistic nature of the ALD coating and the VC that form a cohesive and flexible SEI to compensate for volume expansion while also mitigating side reactions with the lithium salts to substantially increase capacity retention. This approach could potentially be further applied to different composites, without altering the

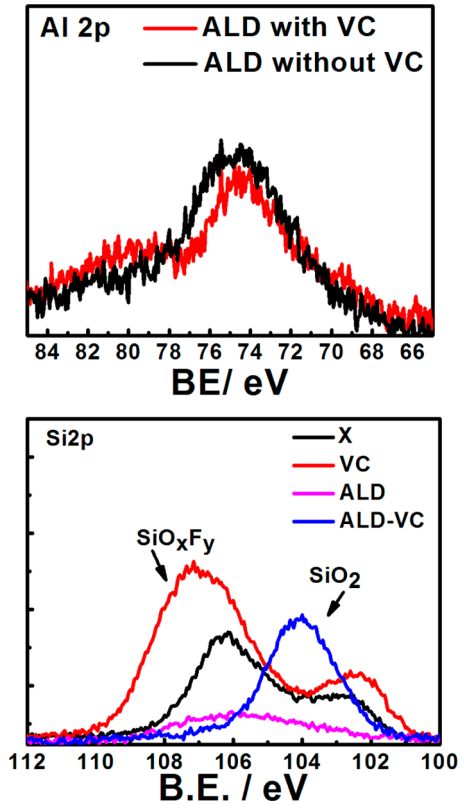

Figure 6. XPS spectra of (top) the Al 2p regions after cycling with and without VC for Al_2O_3 ALD-coated Si−C anodes and (bottom) Si 2p regions after cycling for the different variations.

underlying composite morphology or structure, to increase stability under longer cycling intervals.

4. CONCLUSION

In summary, a highly stable nanosized Si−C composite anode for Li-ion batteries was fabricated by coupling atomic layer deposition coating (placed directly on the anode) with the electrolyte additive VC to form a flexible weblike network and a sufficiently stable solid electrolyte interface that is absent of the

DOI: 10.1021/acsami.5b01853
ACS Appl. Mater. Interfaces 2015, 7, 13801−13807

Scheme 1. Diagram of the Interaction of ALD and VC during Cycling[a]

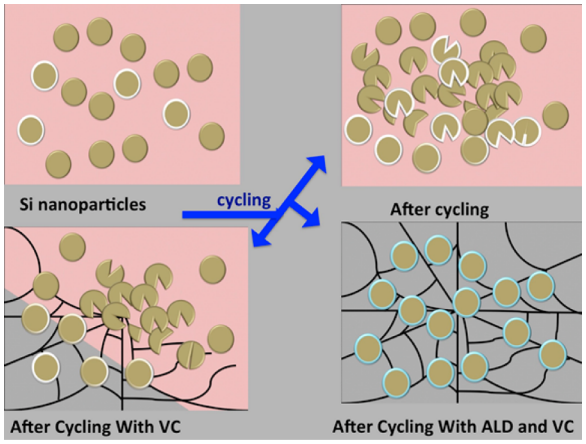

[a]SiO2 is shown as a white coating. After cycling, the bare electrode (top right) shows pulverization and agglomeration of the particles; in VC (bottom left), a small portion of the silicon nanoparticles maintains good dispersion, but most become pulverized and agglomerate. With ALD and VC (bottom right), a different surface forms along with good dispersion throughout.

fluorinated species; these result in the increase of cycle stability over long charging−discharging cycles versus that of the bare electrode without the addition of VC. Although the bare composite anode showed only an improvement from a 56% to a 45% loss after 50 cycles, when VC was introduced, the ALD-coated Si anode showed an improvement from a 73% to an 11% loss. Furthermore, the anode with the ALD coating and VC had a capacity of 630 mAh g^{-1} after 200 cycles running at 200 mA g^{-1}, and the bare anode without VC showed a capacity of 400 mAh g^{-1} after only 50 cycles. The soft post-treatment approach of combining ALD with the electrolyte additive VC can easily be applied to any silicon composite system to overcome the poor cycle stability that is associated with volume changes and nanoparticle agglomeration.

■ ASSOCIATED CONTENT

Supporting Information

SEM and TEM images of Si@C at the pristine and cycled states and for nanosized SI with nanotubes; graphs showing the electrochemical charge−discharge curve for the rGO−CNT electrode and capacity versus cycle number for rGO and rGO−CNT electrodes. The Supporting Information is available free of charge on the ACS Publications website at DOI: 10.1021/acsami.5b01853.

■ AUTHOR INFORMATION

Corresponding Author

*E-mail: bjh@mail.ntust.edu.tw.

Present Address

[‖]Department of NanoEngineering, University of California San Diego La Jolla, CA 92037, United States

Author Contributions

The manuscript was written through contributions of all authors. S.Y. and Y.-H.C. contributed equally. All authors have given approval to the final version of the manuscript.

Notes

The authors declare no competing financial interest.

■ ACKNOWLEDGMENTS

We acknowledge the financial support from the Ministry of Science and Technology (MOST) (103-2221-E-011-156-MY3, 103-3113-E-011−001, 101-3113-E-011-002, 101-2923-E-011-001-MY3), the Ministry of Economic Affairs (MOEA) (101-EC-17-A-08-S1-183),and the Top University Projects of Ministry of Education (MOE) (100H451401) as well as the facilities support from the National Taiwan University of Science and Technology (NTUST).

■ REFERENCES

(1) Su, X.; Wu, Q. L.; Li, J. C.; Xiao, X. C.; Lott, A.; Lu, W. Q.; Sheldon, B. W.; Wu, J. Silicon-Based Nanomaterials for Lithium-Ion Batteries: A Review. *Adv. Energy Mater.* **2014**, *4*, 1300882.

(2) Holzapfel, M.; Buqa, H.; Hardwick, L. J.; Hahn, M.; Würsig, A.; Scheifele, W.; Novák, P.; Kötz, R.; Veit, C.; Petrat, F.-M. Nano Silicon for Lithium-Ion Batteries. *Electrochim. Acta* **2006**, *52*, 973−978.

(3) Ye, Y.-S.; Xie, X.-L.; Rick, J.; Chang, F.-C.; Hwang, B.-J. Improved Anode Materials for Lithium-Ion Batteries Comprise Non-Covalently Bonded Graphene and Silicon Nanoparticles. *J. Power Sources* **2014**, *247*, 991−998.

(4) Martin, L.; Martinez, H.; Ulldemolins, M.; Pecquenard, B.; Le Cras, F. Evolution of the Si Electrode/Electrolyte Interface in Lithium Batteries Characterized by XPS and AFM Techniques: The Influence of Vinylene Carbonate Additive. *Solid State Ionics* **2012**, *215*, 36−44.

(5) Li, C.; Zhang, H.; Fu, L.; Liu, H.; Wu, Y.; Rahm, E.; Holze, R.; Wu, H. Cathode Materials Modified by Surface Coating for Lithium Ion Batteries. *Electrochim. Acta* **2006**, *51*, 3872−3883.

(6) Meng, X.; Yang, X. Q.; Sun, X. Emerging Applications of Atomic Layer Deposition for Lithium-Ion Battery Studies. *Adv. Mater. (Weinheim, Ger.)* **2012**, *24*, 3589−615.

(7) Kohandehghan, A.; Kalisvaart, P.; Cui, K.; Kupsta, M.; Memarzadeh, E.; Mitlin, D. Silicon Nanowire Lithium-Ion Battery Anodes with ALD Deposited Tin Coatings Demonstrate a Major Improvement in Cycling Performance. *J. Mater. Chem. A* **2013**, *1*, 12850.

(8) Lotfabad, E. M.; Kalisvaart, P.; Kohandehghan, A.; Cui, K.; Kupsta, M.; Farbod, B.; Mitlin, D. Si Nanotubes ALD Coated with TiO_2, Tin, or Al_2O_3 as High Performance Lithium Ion Battery Anodes. *J. Mater. Chem. A* **2014**, *2*, 2504.

(9) Chen, L.; Wang, K.; Xie, X.; Xie, J. Effect of Vinylene Carbonate (Vc) as Electrolyte Additive on Electrochemical Performance of Si Film Anode for Lithium Ion Batteries. *J. Power Sources* **2007**, *174*, 538−543.

(10) Hu, Y.-S.; Demir-Cakan, R.; Titirici, M.-M.; Müller, J.-O.; Schlögl, R.; Antonietti, M.; Maier, J. Superior Storage Performance of a Si@SiOx/C Nanocomposite as Anode Material for Lithium-Ion Batteries. *Angew. Chem., Int. Ed.* **2008**, *47*, 1645−1649.

(11) Du, Y.; Zhu, G.; Wang, K.; Wang, Y.; Wang, C.; Xia, Y. Si/Graphene Composite Prepared by Magnesium Thermal Reduction of SiO_2 as Anode Material for Lithium-Ion Batteries. *Electrochem. Commun.* **2013**, *36*, 107−110.

(12) Hy, S.; Felix; Chen, Y.-H.; Liu, J.-y.; Rick, J.; Hwang, B.-J. In Situ Surface Enhanced Raman Spectroscopic Studies of Solid Electrolyte Interphase Formation in Lithium Ion Battery Electrodes. *J. Power Sources* **2014**, *256*, 324−328.

(13) Martin, C.; Crosnier, O.; Retoux, R.; Bélanger, D.; Schleich, D. M.; Brousse, T. Chemical Coupling of Carbon Nanotubes and Silicon Nanoparticles for Improved Negative Electrode Performance in Lithium-Ion Batteries. *Adv. Funct. Mater.* **2011**, *21*, 3524−3530.

(14) Martin, C.; Alias, M.; Christien, F.; Crosnier, O.; Belanger, D.; Brousse, T. Graphite-Grafted Silicon Nanocomposite as a Negative Electrode for Lithium-Ion Batteries. *Adv. Mater. (Weinheim, Ger.)* **2009**, *21*, 4735−4741.

(15) Marcano, D. C.; Kosynkin, D. V.; Berlin, J. M.; Sinitskii, A.; Sun, Z.; Slesarev, A.; Alemany, L. B.; Lu, W.; Tour, J. M. Improved Synthesis of Graphene Oxide. *ACS Nano* **2010**, *4*, 4806−4814.

DOI: 10.1021/acsami.5b01853
ACS Appl. Mater. Interfaces 2015, 7, 13801−13807

(16) Li, J.; Xiao, X.; Cheng, Y.-T.; Verbrugge, M. W. Atomic Layered Coating Enabling Ultrafast Surface Kinetics at Silicon Electrodes in Lithium Ion Batteries. *J. Phys. Chem. Lett.* **2013**, *4*, 3387−3391.
(17) He, Y.; Yu, X.; Wang, Y.; Li, H.; Huang, X. Alumina-Coated Patterned Amorphous Silicon as the Anode for a Lithium-Ion Battery with High Coulombic Efficiency. *Adv. Mater. (Weinheim, Ger.)* **2011**, *23*, 4938−4941.
(18) Xiao, X.; Lu, P.; Ahn, D. Ultrathin Multifunctional Oxide Coatings for Lithium Ion Batteries. *Adv. Mater. (Weinheim, Ger.)* **2011**, *23*, 3911−3915.
(19) Ren, J.-G.; Wu, Q.-H.; Hong, G.; Zhang, W.-J.; Wu, H.; Amine, K.; Yang, J.; Lee, S.-T. Silicon-Graphene Composite Anodes for High-Energy Lithium Batteries. *Energy Technol. (Weinheim, Ger.)* **2013**, *1*, 77−84.
(20) Erickson, E. M.; Ghanty, C.; Aurbach, D. New Horizons for Conventional Lithium Ion Battery Technology. *J. Phys. Chem. Lett.* **2014**, *5*, 3313−3324.
(21) Aurbach, D.; Gamolsky, K.; Markovsky, B.; Gofer, Y.; Schmidt, M.; Heider, U. On the Use of Vinylene Carbonate (VC) as an Additive to Electrolyte Solutions for Li-Ion Batteries. *Electrochim. Acta* **2002**, *47*, 1423−1439.
(22) Philippe, B.; Dedryvère, R.; Gorgoi, M.; Rensmo, H.; Gonbeau, D.; Edström, K. Role of the LiPF6 Salt for the Long-Term Stability of Silicon Electrodes in Li-Ion Batteries − a Photoelectron Spectroscopy Study. *Chem. Mater.* **2013**, *25*, 394−404.
(23) Philippe, B.; Dedryvere, R.; Gorgoi, M.; Rensmo, H.; Gonbeau, D.; Edstrom, K. Improved Performances of Nanosilicon Electrodes Using the Salt LiFSI: A Photoelectron Spectroscopy Study. *J. Am. Chem. Soc.* **2013**, *135*, 9829−9842.

DOI: 10.1021/acsami.5b01853
ACS Appl. Mater. Interfaces 2015, 7, 13801−13807